J|A|C|S ARTICLES

Published on Web 08/11/2009

Hydrogen/Deuterium Exchange Mass Spectrometry with Top-Down Electron Capture Dissociation for Characterizing Structural Transitions of a 17 kDa Protein

Jingxi Pan,[†] Jun Han,[‡] Christoph H. Borchers,[‡] and Lars Konermann*,[†]

Department of Chemistry, The University of Western Ontario, London, ON, N6A 5B7, Canada, and University of Victoria-Genome BC Proteomics Centre, Victoria, BC, V8Z 7X8, Canada

Received June 1, 2009; E-mail: konerman@uwo.ca

Abstract: Amide H/D exchange (HDX) mass spectrometry (MS) is widely used for protein structural studies. Traditionally, this technique involves protein labeling in D_2O, followed by acid quenching, proteolytic digestion, and analysis of peptide deuteration levels by HPLC/MS. There is great interest in the development of alternative HDX approaches involving the top-down fragmentation of electrosprayed protein ions, instead of relying on enzymatic cleavage and solution-phase separations. A number of recent studies have demonstrated that electron capture dissociation (ECD) results in fragmentation of gaseous protein ions with little or no H/D scrambling. However, the successful application of this approach for in-depth protein conformational studies has not yet been demonstrated. The current work uses horse myoglobin as a model system for assessing the suitability of HDX-MS with top-down ECD for experiments of this kind. It is found that ECD can pinpoint the locations of protected amides with an average resolution of less than two residues for this 17 kDa protein. Native holo-myoglobin (hMb) shows considerable protection from exchange in all of its helices, whereas loops are extensively deuterated. Fraying is observable at some helix termini. Removal of the prosthetic heme group from hMb produces apo-myoglobin (aMb). Both hMb and aMb share virtually the same HDX protection pattern in helices A−E, whereas helix F is unfolded in aMb. In addition, destabilization is evident for some residues close to the beginning of helix G, the end of helix H, and the C-terminus of the protein. The structural changes reported herein are largely consistent with earlier NMR data for sperm whale myoglobin, although small differences between the two systems are evident. Our findings demonstrate that the level of structural information obtainable with top-down ECD for small to medium-sized proteins considerably surpasses that of traditional HDX-MS experiments, while at the same time greatly reducing undesired amide back exchange.

Introduction

Amide hydrogen/deuterium exchange (HDX) measurements represent an important avenue for characterizing protein structure and dynamics. These studies are typically carried out under "in-exchange" conditions, that is, by exposing an unlabeled protein to D_2O. In neutral solution and at room temperature, HDX at unprotected backbone amides occurs within less than a second. In contrast, the rate of -CO-NH- → -CO-ND- conversion is reduced by up to 10^8-fold for sites that are hydrogen bonded and/or shielded from the solvent. The slow exchange of these protected hydrogens is mediated by structural fluctuations, that is, unfolding/refolding events that induce the transient disruption of hydrogen bonds and provide solvent access.[1,2] Continuous-labeling HDX experiments provide detailed information on protein dynamics, as well as local and global stability.[3−5] HDX pulse labeling can be employed for obtaining "snapshots" of protein structures, an approach that has been very fruitful for the characterization of short-lived folding intermediates.[6−9]

2D-NMR has long been the method of choice for protein HDX studies, as it reports on the deuteration status of individual amide groups.[2−6,8−10] Alternatively, HDX can be monitored by mass spectrometry (MS), an approach that is being used by a steadily increasing number of researchers.[11−25] In contrast to NMR, MS has greater sensitivity which allows measurements

[†] The University of Western Ontario.
[‡] University of Victoria-Genome BC Proteomics Centre.

(1) Hvidt, A.; Nielsen, S. O. *Adv. Protein Chem.* **1966**, *21*, 287–386.
(2) Krishna, M. M. G.; Hoang, L.; Lin, Y.; Englander, S. W. *Methods* **2004**, *34*, 51–64.
(3) Bai, Y.; Sosnick, T. R.; Mayne, L.; Englander, S. W. *Science* **1995**, *269*, 192–197.
(4) Carulla, N.; Barany, G.; Woodward, C. *Biophys. Chem* **2002**, *101−102*, 67–79.
(5) Parker, M. J.; Marqusee, S. *J. Mol. Biol.* **2001**, *305*, 593–602.
(6) Uzawa, T.; Nishimura, C.; Akiyama, S.; Ishimori, K.; Takahashi, S.; Dyson, H. J.; Wright, P. E. *Proc. Natl. Acad. Sci. U.S.A.* **2008**, *105*, 13859–13864.
(7) Kuwata, K.; Shastry, R.; Cheng, H.; Hoshino, M.; Batt, C. A.; Goto, Y.; Roder, H. *Nat. Struct. Biol.* **2001**, *8*, 151–155.
(8) Roder, H.; Elove, G. A.; Englander, S. W. *Nature* **1988**, *335*, 700–704.
(9) Udgaonkar, J. B.; Baldwin, R. L. *Nature* **1988**, *335*, 694–699.
(10) Hughson, F. M.; Wright, P. E.; Baldwin, R. L. *Science* **1990**, *249*, 1544–1548.
(11) Powell, K. D.; Ghaemmaghami, S.; Wang, M. Z.; Ma, L.; Oas, T. G.; Fitzgerald, M. C. *J. Am. Chem. Soc.* **2002**, *124*, 10256–10257.
(12) Englander, S. W. *J. Am. Soc. Mass Spectrom.* **2006**, *17*, 1481–1489.
(13) Eyles, S. J.; Kaltashov, I. A. *Methods* **2004**, *34*, 88–99.
(14) Lanman, J.; Lam, T. T.; Barnes, S.; Sakalian, M.; Emmett, M. R.; Marshall, A. G.; Prevelige, P. E. *J. Mol. Biol.* **2003**, *325*, 759–772.

at lower protein concentrations. Also, MS can cope with proteins that are beyond the NMR size limit. Additional features of MS include the ability to detect coexisting conformers, and the straightforward distinction between EX1 and EX2 mechanisms.[22,26−29] The traditional HDX-MS workflow encompasses isotope labeling of the protein, followed by acid quenching of the solution at pH 2.5 and 0 °C. Pepsin is then added to induce limited proteolysis. The resulting protein fragments are separated by HPLC and analyzed by electrospray ionization (ESI)-MS. Side chain deuterons undergo rapid back exchange during HPLC, but labeling information is retained for the protein backbone. HDX levels of individual protein segments can be determined from the measured peptide mass shifts.[16,22,30] The spatial resolution of HDX-MS is limited by the size of the proteolytic fragments, often around 10 residues. This resolution can be enhanced somewhat by exploiting data obtained from overlapping peptides, and by using multiple proteases with different cleavage preferences.[31,32] Partial deuterium loss at all backbone amides during analysis is unavoidable, necessitating the use of steep HPLC gradients and the inclusion of suitable controls.[16,22] An aspect that tends to go unnoticed is that enzymatic hydrolysis turns backbone amides into free H_2N-peptide termini that cannot retain their isotope label. In addition, the amide linkages adjacent to each peptide N-terminus undergo back exchange as well.[33] Each cleavage event, therefore, leads to the loss of information for *two* backbone amides.

To enhance the scope and versatility of HDX-MS, considerable efforts have been made to use gas-phase fragmentation techniques instead of (or in combination with) the classical proteolytic digestion approach. A number of studies employing collision-induced dissociation (CID) found fragment deuteration patterns that were partially consistent with the expected solution-phase behavior.[34−40] Unfortunately, several other reports found spatial H/D randomization ("scrambling") after CID.[41−45] The occurrence of scrambling is consistent with the mobile proton model, which stipulates that the formation of *b* and *y″* fragments from vibrationally excited precursor ions involves the rapid intramolecular migration of H^+ or D^+.[46−50] It must be concluded that CID does not represent a generally viable approach for spatially resolved HDX-MS measurements.[41−45]

Electron capture dissociation (ECD) represents an alternative fragmentation technique. Capture of an electron by an even-electron polypeptide cation in the gas phase leads to $N-C_\alpha$ cleavage, producing a $c/z^\bullet$ ion pair.[51−53] Although the ECD mechanism remains a matter of debate,[54] there is considerable evidence that the process is "nonergodic", implying that rapid bond cleavage occurs before the excitation energy is randomized and before H/D scrambling can take place.[51,55] ECD tends to provide a larger sequence coverage than CID, thereby facilitating the analysis of intact proteins in a "top-down" fashion, that is, without prior protease treatment.[56−61] Similar experiments can also be performed with electron transfer dissociation (ETD), which represents a closely related technique.[62,63]

(15) Lu, X.; Wintrode, P. L.; Surewicz, W. K. *Proc. Natl. Acad. Sci. U.S.A.* **2007**, *104*, 1510–1515.
(16) Wales, T. E.; Engen, J. R. *Mass Spectrom. Rev.* **2006**, *25*, 158–170.
(17) Zhu, M. M.; Rempel, D. L.; Du, Z.; Gross, M. L. *J. Am. Chem. Soc.* **2003**, *125*, 5252–5253.
(18) Huzil, J. T.; Chik, J. K.; Slysz, G. W.; Freedman, H.; Tuszynski, J.; Taylor, R. E.; Sackett, D. L.; Schriemer, D. C. *J. Mol. Biol.* **2008**, *378*, 1016–1030.
(19) Chalmers, M. J.; Busby, S. A.; Pascal, B. D.; He, Y.; Hendrickson, C. L.; Marshall, A. G.; Griffin, P. R. *Anal. Chem.* **2006**, *78*, 1005–1014.
(20) Rand, K. D.; Adams, C. M.; Zubarev, R. A.; Jorgensen, T. J. D. *J. Am. Chem. Soc.* **2008**, *130*, 1341–1349.
(21) Rist, W.; Rodriguez, F.; Jorgensen, T. J. D.; Mayer, M. P. *Protein Sci.* **2005**, *14*, 626–632.
(22) Smith, D. L.; Deng, Y.; Zhang, Z. *J. Mass Spectrom.* **1997**, *32*, 135–146.
(23) Maier, C. S.; Deinzer, M. L. *Methods Enzymol.* **2005**, *402*, 312–360.
(24) Truhlar, S. M. E.; Croy, C. H.; Torpey, J. W.; Koeppe, J. R.; Komives, E. A. *J. Am. Soc. Mass Spectrom.* **2006**, *17*, 1490–1497.
(25) Busenlehner, L. S.; Armstrong, R. N. *Arch. Biochem. Biophys.* **2005**, *433*, 34–46.
(26) Kaltashov, I. A.; Eyles, S. J. *Mass Spectrom. Rev.* **2002**, *21*, 37–71.
(27) Miranker, A.; Robinson, C. V.; Radford, S. E.; Aplin, R.; Dobson, C. M. *Science* **1993**, *262*, 896–900.
(28) Konermann, L.; Tong, X.; Pan, Y. *J. Mass Spectrom.* **2008**, *43*, 1021–1036.
(29) Tsui, V.; Garcia, C.; Cavagnero, S.; Siuzdak, G.; Dyson, H. J.; Wright, P. E. *Protein Sci.* **1999**, *8*, 45–49.
(30) Wales, T. E.; Fadgen, K. E.; Gerhardt, G. C.; Engen, J. R. *Anal. Chem.* **2008**, *80*, 6815–6820.
(31) Cravello, L.; Lascoux, D.; Forest, E. *Rapid Commun. Mass Spectrom.* **2003**, *17*, 2387–2393.
(32) Del Mar, C.; Greenbaum, E. A.; Mayne, L.; Englander, S. W.; Woods, V. L., Jr. *Proc. Natl. Acad. Sci. U.S.A.* **2005**, *102*, 15477–15482.
(33) Wang, L.; Smith, D. L. *Anal. Biochem.* **2003**, *314*, 46–53.
(34) Deng, Y.; Pan, H.; Smith, D. L. *J. Am. Chem. Soc.* **1999**, *121*, 1966–1967.
(35) Kim, M.-Y.; Maier, C. S.; Reed, D. J.; Deinzer, M. L. *J. Am. Chem. Soc.* **2001**, *123*, 9860–9866.
(36) Demmers, J. A. A.; Rijkers, D. T. S.; Haverkamp, J.; Killian, J. A.; Heck, A. J. R. *J. Am. Chem. Soc.* **2002**, *124*, 11191–11198.
(37) Anderegg, R. J.; Wagner, D. S.; Stevenson, C. L.; Borchardt, R. T. *J. Am. Soc. Mass Spectrom.* **1994**, *5*, 425–433.
(38) Akashi, S.; Naito, Y.; Takio, K. *Anal. Chem.* **1999**, *71*, 4974–4980.
(39) Eyles, S. J.; Speir, J. P.; Kruppa, G. H.; Gierasch, L. M.; Kaltashov, I. A. *J. Am. Chem. Soc.* **2000**, *122*, 495–500.
(40) Hoerner, J. K.; Xiao, H.; Kaltashov, I. A. *Biochemistry* **2005**, *44*, 11286–11294.
(41) Jørgensen, T. J. D.; Gårdsvoll, H.; Ploug, M.; Roepstorff, P. *J. Am. Chem. Soc.* **2005**, *127*, 2785–2793.
(42) Johnson, R. S.; Krylov, D.; Walsh, K. A. *J. Mass. Spectrom.* **1995**, *30*, 386–387.
(43) McLafferty, F. W.; Guan, Z.; Haupts, U.; Wood, T. D.; Kelleher, N. L. *J. Am. Chem. Soc.* **1998**, *120*, 4732–4740.
(44) Ferguson, P. L.; Pan, J.; Wilson, D. J.; Dempsey, B.; Lajoie, G.; Shilton, B.; Konermann, L. *Anal. Chem.* **2007**, *79*, 153–160.
(45) Ferguson, P. L.; Konermann, L. *Anal. Chem.* **2008**, *80*, 4078–4086.
(46) Dongré, A. R.; Jones, J. L.; SomogyiÁ.; Wysocki, V. H. *J. Am. Chem. Soc.* **1996**, *118*, 8365–8374.
(47) Tang, X.-J.; Thibault, P.; Boyd, R. K. *Anal. Chem.* **1993**, *65*, 2824–2834.
(48) Harrison, A. G.; Yalcin, T. *Int. J. Mass Spectrom.* **1997**, *165/166*, 339–347.
(49) Paizs, B.; Suhai, S. *Mass Spectrom. Rev.* **2005**, *24*, 508–548.
(50) Summerfield, S. G.; Gaskell, S. J. *Int. J. Mass Spectrom.* **1997**, *165/166*, 509–521.
(51) Zubarev, R. A.; Kelleher, N. L.; McLafferty, F. W. *J. Am. Chem. Soc.* **1998**, *120*, 3265–3266.
(52) Zubarev, R. A.; Zubarev, A. R.; Savitski, M. M. *J. Am. Soc. Mass Spectrom.* **2008**, *19*, 753–761.
(53) Coon, J. *J. Anal. Chem.* **2009**, *81*, 3208–3215.
(54) Sohn, C. H.; Chung, C. K.; Yin, S.; Ramachandran, P.; Loo, J. A.; Beauchamp, J. L. *J. Am. Chem. Soc.* **2009**, *131*, 5444–5459.
(55) Breuker, K.; Oh, H.; Lin, C.; Carpenter, B. K.; McLafferty, F. W. *Proc. Natl. Acad. Sci. U.S.A.* **2004**, *101*, 14011–14016.
(56) Cooper, H. J.; Hakansson, K.; Marshall, A. G. *Mass Spectrom. Rev.* **2005**, *24*, 201–222.
(57) Han, X.; Jin, M.; Breuker, K.; McLafferty, F. W. *Science* **2006**, *314*, 109–112.
(58) Siuti, N.; Kelleher, N. L. *Nat. Methods* **2007**, *4*, 817–821.
(59) Sze, S. K.; Ge, Y.; Oh, H.; McLafferty, F. W. *Proc. Natl. Acad. Sci. U.S.A.* **2002**, *99*, 1774–1779.
(60) Ge, Y.; Lawhorn, B. G.; ElNaggar, M.; Strauss, E.; Park, J.-H.; Begley, T. P.; McLafferty, F. W. *J. Am. Chem. Soc.* **2002**, *124*, 672–677.
(61) Xie, Y.; Zhang, J.; Yin, S.; Loo, J. A. *J. Am. Chem. Soc.* **2006**, *128*, 14432–14433.
(62) Molina, H.; Horn, D. M.; Tang, N.; Mathivanan, S.; Pandey, A. *Proc. Natl. Acad. Sci. U.S.A.* **2007**, *104*, 2199–2204.
(63) Syka, J. E. P.; Coon, J. J.; Schroeder, M. J.; Shabanowitz, J.; Hunt, D. F. *Proc. Natl. Acad. Sci. U.S.A.* **2004**, *101*, 9528–9533.

The idea of using ECD or ETD for scrambling-free top-down HDX-MS holds tremendous promise, because such an approach could eliminate proteolysis, HPLC, and amide back-exchange from the experimental workflow, while potentially yielding higher spatial resolution.[64,65] Jørgensen and co-workers recently provided direct proof that ECD[20] and ETD[66,67] are indeed capable of preserving the solution-phase deuteration pattern of short peptides. In related experiments, our group used ECD for the top-down analysis of ubiquitin, a small (8.5 kDa) protein. The deuteration levels of 30 *c* and 19 $z^{\bullet}$ ions were found to be consistent with previous HDX-NMR data.[68] Kaltashov and colleagues analyzed the 18 kDa protein CRABP by ETD after HDX in solution. Only a very limited number of fragment ions could be analyzed in that work, but the results nonetheless provided further support for the general feasibility of top-down HDX-MS measurements.[69]

The primary focus of earlier ECD and ETD-based HDX-MS studies was to prove the absence of scrambling. Despite the encouraging results obtained in this way,[20,51,66,68−70] it remains an open question whether top-down HDX-MS with ECD/ETD is capable of matching (or surpassing) the level of protein structural information that is obtainable by existing proteolytic digestion approaches. Key questions include the effective protein size limit and spatial resolution that is achievable with top-down HDX-MS. Also, it is unclear whether data obtained in this way are adequate for detecting relatively subtle protein conformational changes.

To assess the performance of top-down HDX-MS as a structural biology tool, the current work employs ECD for spatially resolved isotope exchange studies on myoglobin. Both the heme-bound version of this 153 residue protein (holomyoglobin, hMb, 17 568 Da) and the apo form (aMb, 16 952 Da) have been studied extensively.[6,71−81] Native hMb adopts a compact fold that comprises eight α-helices (A−H) which are connected by short loops. The prosthetic heme group is bound in a hydrophobic pocket where it makes numerous noncovalent contacts with the protein, in addition to proximal ligation of the heme iron by H93 in helix F.[77] $^{13}C_{\alpha}$ chemical shift NMR data indicate that the structure of native aMb resembles that of hMb, with the exception that helix F and some of the adjacent regions are disordered.[71,72] The top-down HDX-ECD-MS data of this work provide a detailed view of the hydrogen bonding patterns in hMb and aMb, thereby validating this experimental approach as a tool for structural studies on proteins in solution.

Experimental Section

Materials. Ferri-hMb from horse skeletal muscle and bovine ubiquitin were obtained from Sigma (St. Louis, MO), apo-Mb was prepared by butanone extraction as described in the literature.[82] Bradykinin was purchased from Bachem (King of Prussia, PA). Similar to previous studies,[83−85] this peptide serves as a rapidly exchanging internal HDX standard. D_2O was from Cambridge Isotope Laboratories (Andover, MA). Stock solutions of hMb were extensively dialyzed against 10 mM ammonium acetate at pH 6.8. Stock solutions of aMb were dialyzed against 50 mM acetic acid to avoid precipitation which can take place after extended storage at neutral pH. The pH of these aMb solutions was raised to 6.8 immediately prior to experiments by addition of ammonium hydroxide. When using this procedure, no precipitation was observed.

Hydrogen/Deuterium Pulse Labeling. HDX was carried out using a three-syringe continuous-flow setup with two sequential mixing steps, where D_2O exposure of the protein is followed by acid quenching and online ESI-MS with top-down ECD. The basic design of the device is similar to systems described previously.[68,86] Briefly, syringe 1 was filled with an aqueous solution containing 50 μM protein (hMb or aMb) and 25 μM bradykinin in 10 mM NH_4Ac at pH 6.8. Syringe 2 contained D_2O with 10 mM NH_4Ac, pH_{read} 6.8. Both syringes were connected to a "zero dead volume" mixing tee (Upchurch Scientific, Oak Harbor, WA) by fused silica capillaries (i.d. 100 μm, Polymicro Technologies, Phoenix, AZ). HDX of the protein was initiated by mixing the contents of syringes 1 and 2 at the tee in a 1:4 volume ratio (4 and 16 μL min^{-1}). The outlet of the mixing tee was connected to a 21 cm long "labeling capillary" (i.d. 100 μm), resulting in an average HDX time of 5 s. The outflow of the labeling capillary was mixed at a second tee with quenching solution from syringe 3 (0.4% formic acid in acetonitrile/H_2O/D_2O in a 1:1.8:7.2 volume ratio, pH_{read} 2.0, 20 μL min^{-1}). This solvent composition ensures that the level of side chain deuteration remains constant throughout the mixing sequence, which facilitates the subsequent data analysis (see below). The outlet of the second mixer was connected to a 9 cm long stainless steel ESI capillary (i.d. 100 μm), resulting in an average residence time of 1 s. Exposure of the protein to acidic conditions inside the ESI capillary quenches amide HDX. The level of amide back exchange during this short quenching step is less than 1%.[12] Nonetheless, this time interval is long enough for the protein to undergo extensive unfolding, as well as heme loss in the case of hMb.[87,88] Thus, the solution-phase protein conformation after quenching is independent of the heme binding state during labeling. In addition, the formation of highly positive ESI charge states for unfolded proteins[26] enhances the electron capture cross section.[51] All three syringes were advanced simultaneously by syringe pumps (Harvard Apparatus, Holliston, MA). Prior to acquisition of ECD spectra, the flow setup

(64) Charlebois, J. P.; Patrie, S. M.; Kelleher, N. L. *Anal. Chem.* **2003**, *75*, 3263–3266.
(65) Kweon, H. K.; Hakansson, K. *Analyst* **2006**, *131*, 275–280.
(66) Zehl, M.; Rand, K. D.; Jensen, O. N.; Jørgensen, T. J. D. *J. Am. Chem. Soc.* **2008**, *130*, 17453–17459.
(67) Rand, K. D.; Zehl, M.; Jensen, O. N.; Jørgensen, T. J. D. *Anal. Chem.* **2009**, *81*, 5577–5584.
(68) Pan, J.; Jun, H.; Borchers, C. H.; Konermann, L. *J. Am. Chem. Soc.* **2008**, *130*, 11574–11575.
(69) Abzalimov, R. R.; Kaplan, D. A.; Easterling, M. L.; Kaltashov, I. A. *J. Am. Soc. Mass Spectrom.* **2009**, *20*, 1514–1517.
(70) Stefanowicz, P.; Petry-Podgorska, I.; Kowalewska, K.; Jaremko, L.; Jaremko, M.; Szewczuk, Z. *Biosci. Rep.* Epub Mar 13, 2009. DOI: 10.1042/BSR20090015.
(71) Eliezer, D.; Yao, J.; Dyson, H. J.; Wright, P. E. *Nat. Struct. Biol.* **1998**, *5*, 148–155.
(72) Eliezer, D.; Wright, P. E. *J. Mol. Biol.* **1996**, *263*, 531–538.
(73) Hughson, F. M.; Barrick, D.; Baldwin, R. L. *Biochemistry* **1991**, *30*, 4113–4118.
(74) Jennings, P. A.; Wright, P. E. *Science* **1993**, *262*, 892–896.
(75) Cavagnero, S.; Theriault, Y.; Narula, S. S.; Dyson, H. J.; Wright, P. E. *Protein Sci.* **2000**, *9*, 186–193.
(76) Scott, E. E.; Paster, E. V.; Olson, J. S. *J. Biol. Chem.* **2000**, *275*, 27129–27136.
(77) Evans, S. V.; Brayer, G. D. *J. Mol. Biol.* **1990**, *213*, 885–897.
(78) Frauenfelder, H.; Sligar, S. G.; Wolynes, P. G. *Science* **1991**, *254*, 1598–1603.
(79) Ostermann, A.; Waschipky, R.; Parak, F. G.; Nienhaus, G. U. *Nature* **2000**, *404*, 205–208.
(80) Schmidt, M.; Nienhaus, K.; Pahl, R.; Krasselt, A.; Anderson, S.; Parak, F.; Nienhaus, G. U.; Srajer, V. *Proc. Nat. Acad. Sci. U.S.A.* **2005**, *102*, 11704–11709.
(81) Johnson, R. S.; Walsh, K. A. *Protein Sci.* **1994**, *3*, 2411–2418.
(82) Teale, F. W. J. *Biochim. Biophys. Acta* **1959**, *35*, 543.
(83) Pan, J. X.; Rintala-Dempsey, A.; Li, Y.; Shaw, G. S.; Konermann, L. *Biochemistry* **2006**, *45*, 3005–3013.
(84) Hossain, B. M.; Simmons, D. A.; Konermann, L. *Can. J. Chem.* **2005**, *83*, 1953–1960.
(85) Katta, V.; Chait, B. T. *J. Am. Chem. Soc.* **1993**, *115*, 6317–6321.
(86) Simmons, D. A.; Konermann, L. *Biochemistry* **2002**, *41*, 1906–1914.
(87) Shen, L. L.; Hermans, J. *Biochemistry* **1972**, *11*, 1836–1841.
(88) Konermann, L.; Rosell, F. I.; Mauk, A. G.; Douglas, D. J. *Biochemistry* **1997**, *36*, 6448–6454.

was operated for ca. 1 h to equilibrate the system. Complete equilibration after this time period was evident from the observation of stable HDX levels for both protein and the bradykinin internal standard. All solutions were at room temperature (22 ± 1 °C) throughout the HDX and quenching steps.

Mass Spectrometry. All data were recorded on a 12 T Apex-Qe hybrid Fourier transform-ion cyclotron resonance (FT-ICR) mass spectrometer (Bruker Daltonics, Billerica, MA) equipped with an Apollo II ESI source, a quadruple mass filter, and a hexapole collision cell. The ESI source was operated in positive ion mode at a capillary voltage of 3500 V with a spray shield voltage of 3200 V. The ion sampling interface was operated under relatively gentle conditions (10 V at skimmer 1, 4.8 V at skimmer 2) to reduce collisional activation which might otherwise induce H/D scrambling.[20] The total solution flow rate coming from the mixing setup was 40 μL min^{-1} at a final protein concentration of 5 μM. The N_2 nebulizing and drying gas flow rates were set at 3.0 and 4.0 L min^{-1}, respectively, and the ion transfer capillary temperature was 150 °C. The Ar background pressure within the hexapole collision cell was ca. 1.2×10^{-6} Torr. Survey scan mass spectra were acquired with a collision cell ion accumulation time of 0.2 s, whereas ECD data were recorded with an accumulation time of 0.5−1 s. The source ion accumulation time was 0.1 s. ECD experiments were performed without precursor selection, that is, by fragmenting the entire ion population within the ICR cell. To increase sequence coverage, each spectrum represents the sum of data acquired under a range of different ECD conditions. The parameters chosen were as follows: heater current through the dispenser cathode filament 1.2−1.4 A, electron pulse length 8−12 ms, electron beam bias 1.2−1.4 V. The grid potential that guides electrons into the ICR cell was between 12 and 15 V. Up to 4000 scans were accumulated over the *m*/*z* range 250−2800, corresponding to an acquisition time of ca. 90 min for each ECD spectrum. The survey scan and ECD operation modes were calibrated with multiply charged ions and fragments, respectively, of ubiquitin.

Data Analysis. Neutral aMb contains 261 exchangeable hydrogens. Of these, 148 are amide backbone hydrogens, 110 are on amino acid side chains, and 3 on the termini.[86] Fragment ion charge states used for data analysis were 1+ for c_3-c_{21} and z_3-z_8, 2+ for $c_{22}-c_{40}$ and z_9-z_{18}, 3+ for $c_{41}-c_{44}$ and $z_{21}-z_{29}$, 4+ for $c_{45}-c_{59}$ and z_{32}, 5+ for c_{66} and $z_{36}-z_{60}$, 6+ for c_{86} and z_{75}, 7+ for $c_{62}-c_{73}$ and z_{68}, 8+ for $c_{78}-c_{83}$ and z_{67}, z_{70}, 9+ for c_{93}, and 10+ for c_{98}. Centroid *m*/*z* values (R) were determined for all c and $z^\bullet$ fragments after isotope exchange in a semiautomated fashion by using HX-Express.[89] Centroid *m*/*z* values for the corresponding unlabeled ions (R_0) were obtained from ProteinProspector (http://prospector.ucsf.edu). The number of protected hydrogens N_{prot} in each fragment ion can be calculated as

$$N_{prot} = N_{tot} - N_{exch} \quad (1)$$

where N_{tot} is the number of exchangeable hydrogens. N_{exch} is the normalized number of exchanged hydrogens that is given by

$$N_{exch} = \frac{n(R - R_0)}{P(m_D - m_H)} - n \quad (2)$$

All three values, N_{prot}, N_{tot}, and N_{exch} include amide backbone, side chain, and terminal sites in the fragment ions, whereas charge carriers are excluded. The parameter n in eq 2 is the charge state of the ion, $m_D = 2.0141$ amu is the atomic mass of deuterium, and $m_H = 1.0078$ amu is the mass of hydrogen. The deuteration level of the bradykinin internal standard (P) was found to be 75.5%, which is slightly lower than the expected value of 80%. This effect may be caused by minor imperfections of the online flow/mixing system. This small deviation is compensated by including the normalization factor P in eq 2. P was determined from the experimental data using an isotope modeling strategy described previously.[44,84]

From the N_{prot} values of eq 1, the locations of hydrogen and deuterium atoms along the amide backbone can be determined. We define the deuteration level D of a backbone amide as $D = 1$ if the site is completely deuterated (lack of protection), and $D = 0$ if the site exclusively carries hydrogen (fully protected). Fractional values of D correspond to partial exchange. For the analysis, it is assumed that exchangeable side chain sites are uniformly labeled to the same level P as the internal standard during the quenching step.[33] It has to be considered that the ion c_q encompasses the amide hydrogen sites of residues 2 to $q + 1$ (residue 1 has no amide linkage but a free amino group instead).[90] Accordingly, the deuteration level of residue 2 (the first backbone amide in the chain) is given by

$$D_2 = 1 - N_{prot}(c_1) \quad (3)$$

For all subsequent c ions, the deuteration level D_q can be calculated as

$$D_q = 1 - (N_{prot}(c_{q-1}) - N_{prot}(c_{q-2})) \quad (4)$$

In cases where ions are missing from the consecutive series of c fragments, one can assign an average deuteration value D_{av} to each of the intervening amide groups. Assume that c_r is detectable, but c_{r+1}, c_{r+2}, ..., are missing from the series all the way to the next detectable ion c_q. The average deuteration level in this case is given by

$$D_{av} = D_{r+2} = \ldots = D_{q+1} = 1 - \frac{N_{prot}(c_q) - N_{prot}(c_r)}{\text{number of amides}(c_q) - \text{number of amides}(c_r)} \quad (5)$$

This strategy includes the special case of X-Pro linkages which do not have an amide hydrogen, and which do not undergo ECD.[91] A framework analogous to eqs 3−5 applies in the case of $z^\bullet$ ions, noting that in myoglobin the ion z_q contains the amide sites of residues $(153 - q + 2)$ to 153.

Results and Discussion

HDX-MS with top-down ECD was used to characterize the spatial H/D distribution in native hMb and aMb. A relatively short (5 s) labeling pulse was chosen prior to acid quenching in order to facilitate the differentiation of protected and unprotected backbone amides. Five seconds is sufficient for the complete exchange of solvent exposed sites that do not participate in stable intramolecular hydrogen bonds. On the other hand, amides that are protected through H-bond formation will undergo only minimal labeling under these conditions.[92] The quenching step was kept very short (1 s) in order to suppress amide back exchange. ECD provides extensive sequence coverage, yielding 46 c and 36 $z^\bullet$ ion signals that were included for the analysis. These fragments cover the entire protein backbone in a partially overlapping fashion (Figure 1). A number of additional c and $z^\bullet$ signals were detectable, but those fragments could not be considered due to their limited S/N ratio.

Top-down ECD after HDX. The overall HDX-induced mass shift is considerably larger for aMb than for hMb (Figure 2A,B), indicating that heme removal leads to a protein conformation

(89) Weis, D. D.; Engen, J. R.; Kass, I. J. *J. Am. Soc. Mass Spectrom.* **2006**, *17*, 1700–1703.
(90) Roepstorff, P. *Biomedical Mass Spectrometry* **1984**, *11*, 601.
(91) Leymarie, N.; Berg, E. A.; McComb, M. E.; O'Connor, P. B.; Grogan, J.; Oppenheim, F. G.; Costello, C. E. *Anal. Chem.* **2002**, *74*, 4124–4132.
(92) Bai, Y.; Milne, J. S.; Mayne, L.; Englander, S. W. *Proteins: Struct. Funct. Genet.* **1993**, *17*, 75–86.

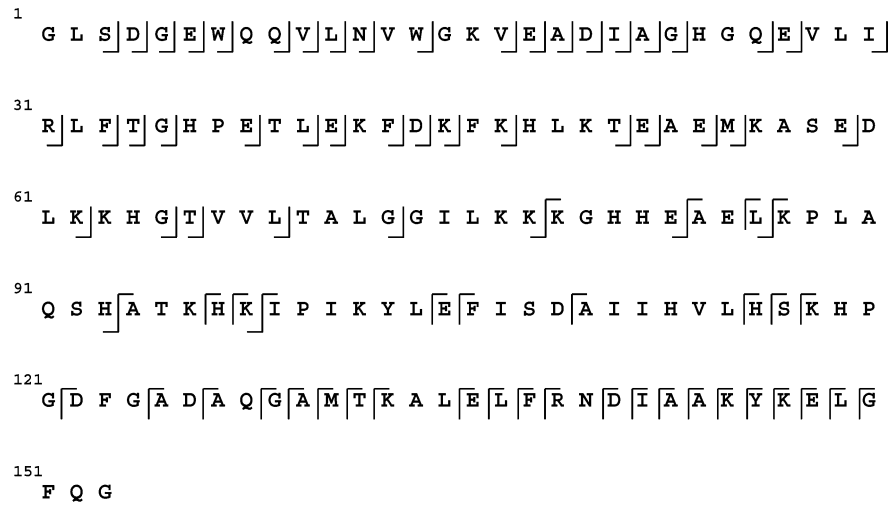

Figure 1. Sequence of horse myoglobin.[77] ECD sites corresponding to N-terminal fragments (*c* ions) and C-terminal fragments ($z^{\bullet}$ ions) that were used for HDX analyses are indicated.

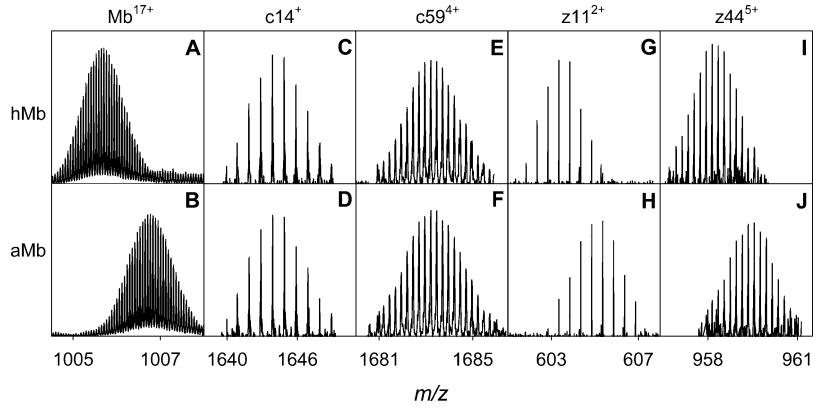

Figure 2. Partial ESI-FT-ICR mass spectra obtained after pulsed HDX of hMb (top row) and aMb (bottom row). Panels A and B are for the intact protein in the 17+ charge state. Also shown are data for several top-down ECD fragments, c_{14}^{+} (C and D), c_{59}^{4+} (E and F), z_{11}^{2+} (G and H), and z_{44}^{5+} (I and J).

that has an increased number of unprotected hydrogens. This finding is consistent with the results of previous work.[71,73,81] Remarkably, the HDX behavior of N-terminal fragments up to c_{83} is very similar for hMb and aMb, despite the vastly different precursor deuteration. This is illustrated for two representative *c* ions in Figure 2C,D and E,F. In contrast, fragments covering regions more toward the C-terminus are considerably more deuterated for aMb than for hMb (Figure 2G,H and I,J). Even without a detailed analysis, two important points are immediately evident from these observations. (i) In the case of extensive H/D scrambling, *all* of the aMb fragment ions would display higher deuteration levels than those from hMb. Hence, the experimental observation of virtually identical mass shifts for many aMb and hMb fragments demonstrates that little (if any) scrambling occurs under the conditions of our work. This finding supports the results of previous investigations on the suitability of ECD for spatially resolved HDX studies.[20,51,68] (ii) The fact that aMb and hMb share very similar hydrogen protection characteristics for their first ~84 residues implies that heme removal leaves this region (encompassing helices A−E[77]) relatively unaffected.

Deuteration Behavior of Fragment Ions. The number of protected hydrogens (N_{prot}) in each of the myoglobin *c* and $z^{\bullet}$ ions can be determined on the basis of eqs 1, 2. The results obtained in this way are summarized in Figure 3. Regions where the experimental N_{prot} profiles exhibit a slope of unity correspond to protein segments that have all of their amide sites completely protected. Conversely, horizontal regions correspond to segments that do not possess any protected hydrogens. A slope between zero and unity signifies partial deuteration. Close inspection of the experimental data in Figure 3A reveals a single instance where the slope exceeds unity ($c_{30} \rightarrow c_{31}$, $\Delta N_{prot} \approx 2.0$). As discussed below, this behavior represents a special case involving a protected side chain hydrogen. For illustrative purposes, Figure 3 also contains N_{prot} plots for the hypothetical case where *all* amide hydrogens in the protein are completely protected (blue solid lines, slope = 1.0). Gaps and lateral shifts in these plots reflect the lack of X-Pro fragmentation during ECD,[91] as well as the absence of amide hydrogens at these linkages.

When applying eq 1 to the mass distributions of intact hMb and aMb (Figures 2A,B), it is found that the former contains a total of $N_{prot} = 109.6$ protected hydrogens, whereas the corresponding number for aMb is 85.0. Alternatively, N_{prot} for the intact proteins can be determined from Figure 3 on the basis of protection data for complementary $c/z^{\bullet}$ ion pairs. This second method provides average N_{prot} values of 110.4 and 86.4 for hMb and aMb, respectively. The excellent agreement of the two approaches attests to the internal consistency of the data as well as the analysis strategy.

Locations of Protected Hydrogens. The spatial H/D distribution within hMb and aMb can be determined on the basis of the N_{prot} data in Figure 3 and eqs 3−5. The amide deuteration

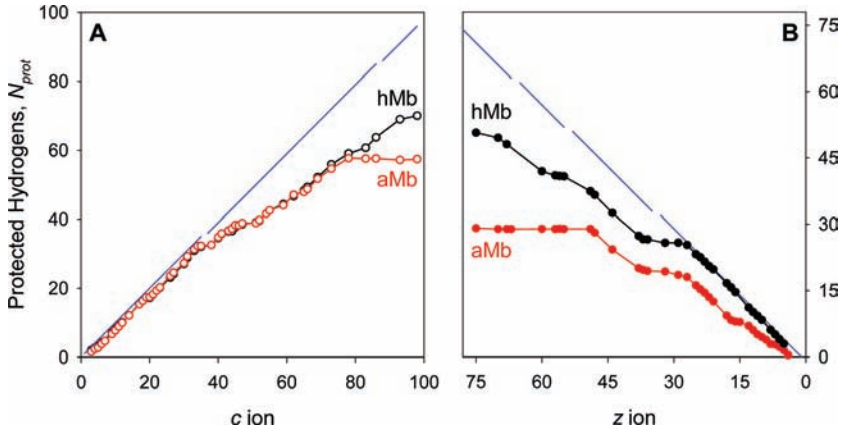

Figure 3. Number of protected hydrogen atoms (N_{prot}) in *c* ions (A) and $z^{\bullet}$ ions (B). Data for hMb are in black, those for aMb are in red. Blue lines represent the hypothetical scenario where every residue carries one protected backbone hydrogen, gaps are due to proline (residues 37, 88, 100, and 120).

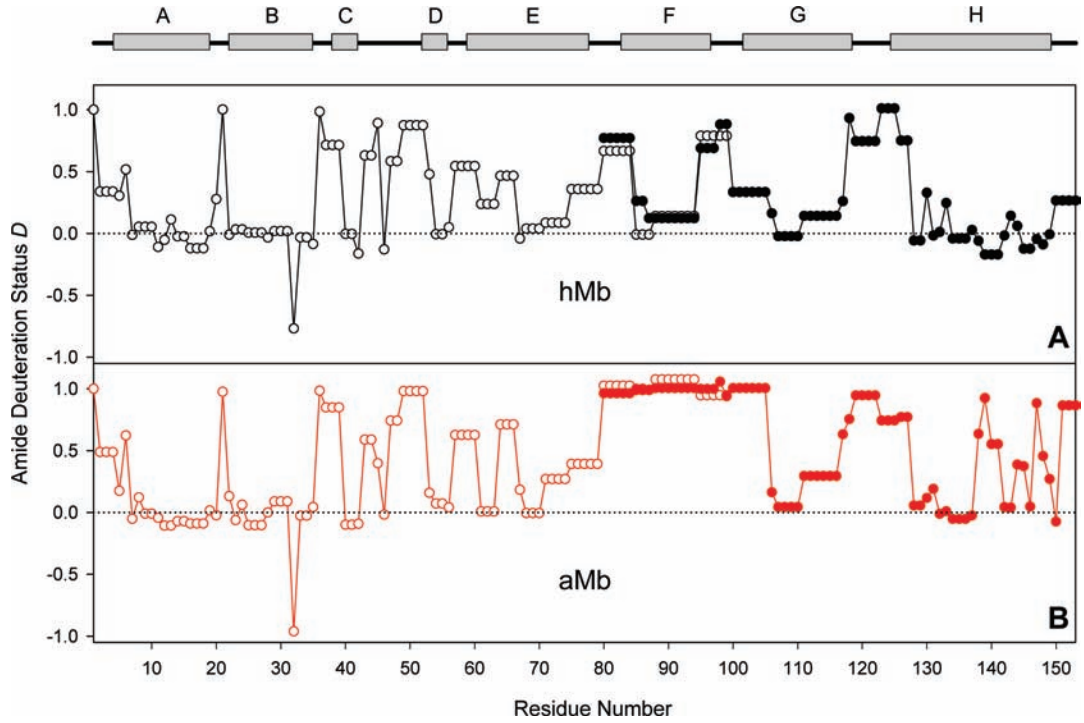

Figure 4. Deuteration status of backbone amide sites in hMb (A) and aMb (B). Open and closed symbols represent data obtained from *c* and $z^{\bullet}$ ions, respectively. The secondary structure of hMb with its eight helices A−H and intervening loops is displayed along the top of the Figure (pdb code 1wla).[77]

status *D* obtained in this way is plotted versus residue number in Figure 4. As outlined in the Experimental Section, $D = 0$ corresponds to a lack of deuteration at a given amide, that is, complete protection. Conversely, $D = 1$ represents the case where an amide site is fully deuterated. Single-residue resolution is obtained for most amides within the first 40 and the last 30 residues. Segments located more toward the center of the sequence are covered with a resolution of two to seven residues. On the basis of repeat measurements, the error in the *D* values of Figure 4 can be estimated to be on the order of ±0.1. This matches the level of agreement between complementary *c* and $z^{\bullet}$ fragment data for residues 80−99, a region where redundant information is obtained.

The hMb data in Figure 4A reveal a clear correlation between the deuteration status measured by HDX-MS and the secondary structure determined by X-ray crystallography.[77] Residues with *D*-values close to zero are generally found within α-helices. Most residues in loop regions show extensive deuteration with *D* values in the range of 0.7 to unity. A visualization of these data is provided in Figure 5A, where the measured HDX behavior has been mapped to the hMb X-ray structure using a three-bin coloring scheme (blue, low deuteration; green, intermediate; red, high). Interestingly, not all residues within helical regions are protected to the same extent. For example, helices E and G exhibit more pronounced deuteration in their N- and C-termini than in the helix center. Similar helix fraying phenomena have previously been observed for other systems.[93] The deuteration pattern uncovered in this work for horse hMb resembles the results of previous HDX-NMR work on sperm whale hMb.[75] The two proteins share the same tertiary fold and have 88% sequence identity.

(93) Fesinmeyer, R. M.; Peterson, E. S.; Dyer, R. B.; Andersen, N. H. *Protein Sci.* **2000**, *14*, 2324–2332.

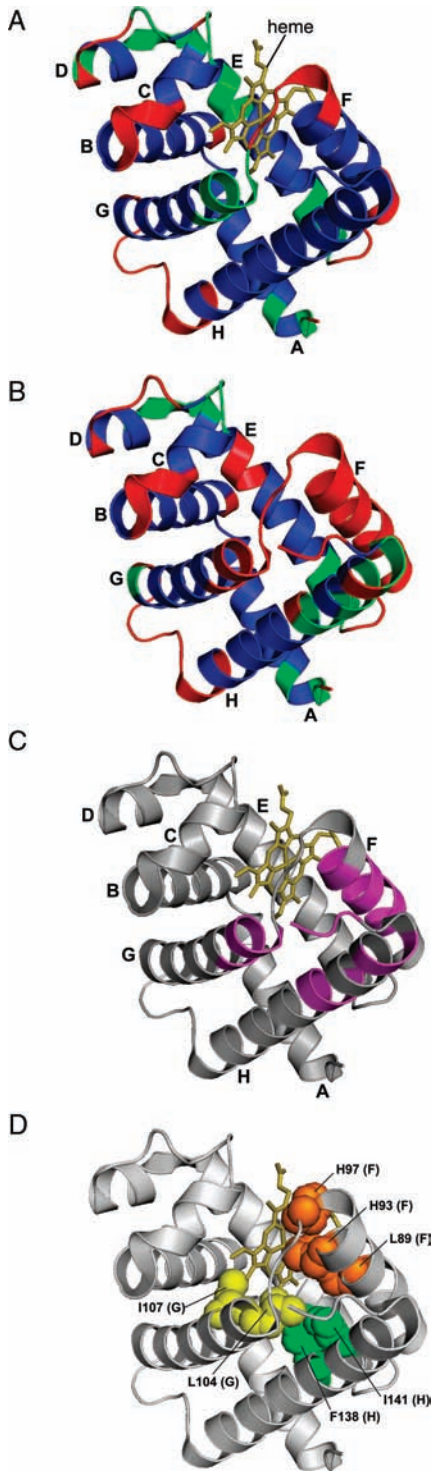

Figure 5. Visualization of the hMb (A) and aMb (B) pulsed HDX behavior. Deuteration levels D are color coded as follows: blue, low (<0.33); green, intermediate (0.33−0.66); red, high (>0.66). Panels A and B are based on the data in Figure 4A and B, respectively. (C) Regions exhibiting the largest HDX differences between aMb and hMb ($\Delta D > 0.5$) are highlighted in magenta. (D) Depiction of side chains in helices F−H that are in direct contact with the heme in hMb. Note the close correlation between the locations of these residues with the magenta-colored helical regions in panel C. In the absence of an experimental 3D structure of aMb, all panels in this Figure are based on the coordinates of hMb.[77]

One particularly interesting feature is the behavior of F46. Despite being part of the extended CD loop, this residue is highly protected in both hMb and aMb (Figure 4A,B). Inspection of the hMb X-ray structure[77] confirms the presence of a hydrogen bond between the amide hydrogen of F46 with the backbone carbonyl of F43 in the same loop. We attribute the particular stability of this loop interaction to participation of the F46, F43, and F33 side chains in a hydrophobic cluster.[77] Formation of this cluster appears to rigidify the positions of F46 and F43, such that formation of a stable amide hydrogen bond becomes possible. Identification of this feature illustrates the level of detail that is achievable with the top-down ECD approach used here.

As noted above, the protection or deprotection of backbone amide hydrogens results in D values between zero and unity in Figure 4. There is a single data point that falls far outside this range. The hMb deuteration level obtained for L32 is −0.77, whereas the result for aMb is −0.96. This observation is attributed to protection of the L32 amide, in addition to a protected side chain hydrogen on R31 (both sites are included in fragment c_{31}). Side chain protection is usually not detectable in HDX-MS due to rapid isotope equilibration with the quenching solution.[16] The only exception is NδH on arginine which undergoes relatively slow back exchange at acidic pH.[81,92] X-ray data confirm the presence of a hydrogen bond between the R31 and H113 side chains.[77] However, while the X-ray structure suggests that a terminal N−H on R31 acts as hydrogen bond donor, our HDX-MS data clearly point to NδH as the protected site. This minor discrepancy may reflect a difference between the solution-phase and the crystal structure of the protein. Except for this single side chain contribution, the D-value progressions of Figure 4 are attributed exclusively to the deuteration status of backbone amides.

Structural Differences between hMb and aMb. The hMb and aMb deuteration progressions are remarkably similar throughout the range covering residues 1−84 (Figure 4A,B). It can be concluded that heme removal has only very minor structural implications for the regions encompassing helices A−E. This finding is in accord with previous NMR work,[71,72] and argues against earlier proposals[94] of major structural changes throughout the entire protein after heme loss. In contrast, Figure 4 reveals numerous major deuteration differences throughout residues 85−153. Most importantly, the entire helix F and the N-terminal backbone amides of helix G are fully deuterated in aMb, indicating that these sections become extensively disordered after heme removal. A similar behavior was found in $^{13}C_\alpha$ chemical shift NMR experiments on sperm whale aMb.[71,72] Different from those data, however, our work shows that heme removal from horse hMb also leads to deprotection of several amides in the C-terminal half of helix H, and for residues 151−153 (Figure 4B, 5B).

Regions that show the largest HDX differences between horse aMb and hMb ($\Delta D > 0.5$) are highlighted in Figure 5C. Most of these segments directly participate in heme−protein interactions (Figure 5D). L89 (helix F), L104 and I107 (helix G), as well as F138 and I141 (helix H) are part of the hydrophobic heme binding pocket in hMb. H93 (helix F) represents the proximal heme iron ligand, whereas the H97 side chain (helix F) forms a hydrogen bond with a heme propionate. While the hMb C-terminus (residues 151−153) is not in direct contact with the heme, it forms a hydrogen bonding network with the magenta-colored helical regions of Figure 5C.[77] Thus, it is not surprising that local unfolding of those helical elements also

(94) Lin, L.; Pinker, R. J.; Forde, K.; Rose, G. D.; Kallenbach, N. R. *Nat. Struct. Biol.* **1994**, *1*, 447–452.

leads to amide deprotection for residues 151−153. Overall, the structural differences between hMb and aMb observed here reveal that heme−protein interactions play a major role in stabilizing the polypeptide fold on the proximal side of the cofactor. The particular vulnerability of helix F is attributable to the presence of P88 which tends to act as a helix breaker.[95] In addition, helix F in hMb is somewhat separated from the rest of the protein by the heme group, such that it cannot make as many contacts with other structural elements.[72,77]

Conclusions

Previous experiments from various laboratories have shown that ECD[20,51,68,70] (as well as ETD[66,67,69]) allows protein fragmentation without H/D scrambling. The current work builds on the foundation provided by those studies, by using HDX-MS with top-down ECD for conducting a detailed structural characterization of a protein in solution. The HDX pattern of native hMb reveals strong protection in α-helical regions, whereas loops are almost completely deuterated. Heme removal induces unfolding of helix F. The beginning of helix G, the end of helix H, and the protein C-terminus (residues 151−153) become destabilized as well. In contrast, the integrity of helices A−E is largely independent of the cofactor. The structural changes upon heme removal seen here for horse myoglobin resemble those reported earlier for the sperm whale protein,[71,72] although some differences between the two variants are evident as well. Our data clearly highlight the feasibility of using HDX-MS with top-down ECD for detecting local changes in protein conformation. For the first time, the current work validates this combination of solution-phase and gas-phase chemistry as a tool for the in-depth characterization of biomolecular structures.

The analyses of this work are based on the deuteration levels of 82 fragments derived from a 17 kDa (153 residue) protein, corresponding to an average spatial resolution of less than two residues. This resolution is far beyond that achievable in traditional MS-based HDX experiments.[81] In addition, the top-down approach employed here does not require digestion and HPLC steps, thereby eliminating back exchange at amides and proteolytically generated peptide amino termini. It remains an advantage of the conventional proteolysis-based HDX-MS technique that it can be applied to proteins which are too large for current top-down techniques (and for NMR). However, rapid advances in FT-ICR technology, in particular the use of stronger magnets, will help mitigate existing size limitations for top-down ECD studies.[57,96,97]

An exciting future extension of the technique used in this work is the combination of top-down ECD with precursor ion selection after HDX. Because different protein structures are often distinguishable by their ESI charge states,[26] the fragmentation of selected precursor ions after labeling could provide highly specific information on individual protein conformers, without interference from coexisting species. The combination of this approach with online rapid mixing techniques[83] should provide an exciting novel opportunity for deciphering protein folding mechanisms.

Acknowledgment. This work was supported by the Natural Sciences and Engineering Council of Canada, the Canada Foundation for Innovation, Genome Canada, Genome BC, and the Canada Research Chairs Program.

JA904379W

(95) Creighton, T. E. *Proteins*; W. H. Freeman & Co: New York, 1993.
(96) Marshall, A. G.; Guan, S. *Rapid Commun. Mass Spectrom.* **1996**, *10*, 1819–1823.
(97) Schaub, T. M.; Hendrickson, C. L.; Horning, S.; Quinn, J. P.; Senko, M. W.; Marshall, A. G. *Anal. Chem.* **2008**, *80*, 3985–3990.